applied optics

Optimal configurations for different incident polarization states in linear polarization calibration

Xinkai Li,[1,2] Bo Chen,[1,*] Lingping He,[1] and Xingjun Gao[1,2]

[1]Changchun Institute of Optics, Fine Mechanics and Physics, Chinese Academy of Sciences, Changchun 130033, China
[2]University of Chinese Academy of Sciences, Beijing 100049, China
*Corresponding author: chen_bo_2019@163.com

Received 24 July 2020; revised 15 September 2020; accepted 16 September 2020; posted 17 September 2020 (Doc. ID 403647); published 19 October 2020

The purpose of polarization calibration is to measure the response matrix of an instrument and the deviation of noise to correct for subsequent flight measurements. The precision, however, is relative to the states of incident light. We investigate the influence of partially polarized light, in the presence of signal-independent additive noise or signal-dependent Poisson shot noise. We obtain the estimation precision for different numbers of the polarization state generators and analyzers in linear Stokes measurements. To reduce the influence of incident light, we suggest that the numbers of the polarization state generators and analyzers should be greater than or equal to 4. In particular, for an instrument including three polarizers oriented at 0°, 60°, and 120°, estimation precision is found to be dependent on the response matrix and incident polarization states.

https://doi.org/10.1364/AO.403647

1. INTRODUCTION

Polarization imaging technology is generally used for noncontact measurements in many fields related to physics, including astronomy [1–4], biology [5–7], medicine [6,8], and the military field [9]. Astronomical observation, especially research for the Sun, holds a dominant position, and polarimetry is a powerful tool for the interpretation of the role of the coronal plasma in the energy transfer process from the inner parts of the Sun to outer space. Especially for a space-based polarimetric instrument, the three first elements of the Stokes vector are sufficient, with circular polarized light considered negligible [10]. A linear polarimetric instrument based on time-division containing three polarizers oriented at 0°, +60°, and −60° cannot be used to realize minimization and equalization of the noise variance [11]. Moreover, if an imaging polarimeter with a large aperture is calibrated, the edge of the incident light produces a degree of linear polarization (DoLP) of at least 1%–5%, which influences the calibration precision for different instruments and configurations. In the past, there has been no analytical method of precision in the presence of Gaussian and Poisson noise. The minimum estimation variance has been studied widely recently [12–17], and it is possible to search the configurations that are stable to incident light.

Reference [18] has found that the distribution of the optimal analysis states is described by a regular polygon. They have established the equivalence of an optimization based on equally weighted variance and the condition number κ of the associated response matrix. In recent years, Goudail proposed a method that can analyze the estimation precision in the presence of Gaussian and Poisson noise [19] and provided closed-form expressions of the estimation variance matrix. They also proposed a set of polarization states depending on the observed Mueller matrix only through its intensity reflectivity, not its other polarimetric properties in the full polarization frame [20]. Reference [12] has derived the optimal reference polarization states, and the analytical results obtained were verified by the simulations and experiments.

By considering the linear polarization calibration, we obtain the estimation variances for the response matrix; the optimal configurations that can minimize and equalize the noise variance are based on the angles satisfying uniform distribution from 0° to 180° [18,21,22]. Moreover, the closed-form expressions for the estimation precision for different incident polarization states are derived, and the estimation variance can exhibit the influence of incident polarization states and the number of measurements. The results show that the numbers of polarization state generators (PSGs) and analyzers employed for linear polarization calibration should be greater than or equal to 4. If the number of generators is 4 and the number of analyzers is 3, the estimation precision is dependent on the response matrix and incident polarization states. We verify this conclusion with Monte Carlo simulations and experiments.

The paper is organized as follows: In Section 2, we describe the linear Stokes calibration and summarize the configurations that optimize the numbers of PSGs and polarization state analyzers (PSAs). Then, we analyze the influence of the incident polarization states in the presence of two types of noise. In Section 3, we present the Monte Carlo simulations for the configurations above. The experimental results, discussions and systematic errors for the linear Stokes calibration are presented in Section 4. Finally, we conclude this paper in Section 5.

2. ESTIMATION PRECISION FOR LINEAR POLARIZATION CALIBRATION

A. Calibration Model of Incident Light

The Mueller matrix used for linear polarization does not consider the circular polarization, and we use the sub-matrix of Mueller matrix that has dimensions 3×3 as

$$M = \begin{pmatrix} M_{11} & M_{12} & M_{13} \\ M_{21} & M_{22} & M_{23} \\ M_{31} & M_{32} & M_{33} \end{pmatrix}. \tag{1}$$

The intensities acquired from source are given by

$$I = I_0 B M A_S^T. \tag{2}$$

The formulation is composed of a light source of intensity I_0, a PSG, which illuminates the optical system, a matrix M, which represents the response of the optical system to any incident linear polarization states, and a PSA that is used to analyze the polarization states of the light generated by the instrument. A detector is used to collect the light exiting from the PSA in a particular direction. I is a $N_B \times N_A$ matrix containing the intensities, which depends on the measurements obtained from the combination of PSA and PSG. The normalized Stokes vector of incident light before PSG is $S = [1; S_1; S_2]$, and the DoLP is $\sqrt{S_1^2 + S_2^2}$. A_{Si}^T can be obtained as

$$A_{Si}^T = A_i \begin{pmatrix} 1 \\ S_1 \\ S_2 \end{pmatrix}. \tag{3}$$

A_i represents the linear polarizer sub-matrix of ith measurement, and we assume that the polarizer is perfect to simplify the calculations as [19,20]

$$A_i = \frac{1}{2} \begin{pmatrix} 1 & \cos 2\theta_i & \sin 2\theta_i \\ \cos 2\theta_i & \cos^2 2\theta_i & \sin 2\theta_i \cos 2\theta_i \\ \sin 2\theta_i & \sin 2\theta_i \cos 2\theta_i & \sin^2 2\theta_i \end{pmatrix}, \tag{4}$$

where θ represents the angles of polarizer in measurements, and $\theta_i = \theta_0 + (i-1) \times 180°/N_A$, and i varies from 1 to N_A. We choose this configuration with $\theta_0 = 0°$. The matrix B, which has dimensions $N_B \times 3$, is stacked row-wise by the first row of analyzer matrix. A_{Si}^T can be rewritten by substituting Eq. (4) into Eq. (3),

$$A_{Si}^T = \begin{pmatrix} 1 + S_1 \cos 2\theta_i + S_2 \sin 2\theta_i \\ \cos 2\theta_i + S_1 \cos^2 2\theta_i + S_2 \sin 2\theta_i \cos 2\theta_i \\ \sin 2\theta_i + S_1 \sin 2\theta_i \cos 2\theta_i + S_2 \sin^2 2\theta_i \end{pmatrix}, \tag{5}$$

where $i \in [1, N_A]$. We can obtain A_S^T, which is a combination of A_{Si}^T,

$$A_S^T = \left(A_{S1}^T, A_{S2}^T, \cdots, A_{SN_A}^T\right), \tag{6}$$

and the matrix A_S^T has the dimensions $3 \times N_A$.

B. Gaussian Noise

To obtain the relationship between I and M, Eq. (2) has been rewritten as follows [20,23]:

$$\mathbf{V}_I = [B \otimes A_S]\mathbf{V}_M, \tag{7}$$

where $\otimes$ denotes the Kronecker product [11], $\mathbf{V}_M = [(V_M)_1\ (V_M)_2 \cdots (V_M)_9]$ is a nine-dimensional vector, and $\mathbf{V}_I = [(V_I)_1\ (V_I)_2 \cdots (V_I)_{N_A N_B}]$ is a $N_A \times N_B$ -dimensional vector. $\mathbf{V}_M$ and $\mathbf{V}_I$ are obtained by reading the matrices M and I in the lexicographic order, respectively.

The influences of the incident polarization states are investigated on the optimal calibration methods with additive Gaussian noise and Poisson shot noise. The pseudo-inverse method is used to describe the estimator from Eq. (7),

$$\mathbf{V}_M = P\mathbf{V}_I, \tag{8}$$

with

$$P = ([B \otimes A_S]^T [B \otimes A_S])^{-1} [B \otimes A_S]^T, \tag{9}$$

where P is the pseudo-inverse of the $9 \times N_A N_B$ -dimensional matrix. Based on the properties of the Kronecker product, the P matrix is rewritten as

$$P = [(G_B)^{-1} \otimes (G_{A_S})^{-1}][B \otimes A_S]^T, \tag{10}$$

where $G_U = U^T U$, with $U = A_S$ or B. We assume that additive Gaussian noise is zero-mean value with variance σ^2. Its covariance matrix can be determined by [20]

$$\Gamma_{\mathbf{V}_M} = \left\langle \mathbf{V}_M \mathbf{V}_M^T \right\rangle - \langle \mathbf{V}_M \rangle^2 = P \Gamma_{\mathbf{V}_I} P^T, \tag{11}$$

where $\langle \cdot \rangle$ denotes ensemble averaging. $\Gamma_{\mathbf{V}_I}$ is the covariance matrix of $\mathbf{V}_I$, and the covariance matrix $\Gamma_{\mathbf{V}_I} = \sigma^2 I$, where I is the $N_A N_B \times N_A N_B$ identity matrix. In this case, the covariance matrix of the response matrix is

$$\Gamma_{\mathbf{V}_M} = \sigma^2 [(G_{A_S})^{-1} \otimes (G_B)^{-1}]. \tag{12}$$

The optimal sets of generator and analyzer polarization states form a regular polygon, and we will use the configurations later. If the incident Stokes vector $S = [1; 0; 0]$, G_{A_S} can be obtained from Eq. (6) as [18]

$$G_{A_S(B)} = \frac{N_{A(B)}}{4} \mathrm{diag}(1, 0.5, 0.5), \tag{13}$$

where $A_S(B)$ has $N_{A(B)} \times 3$ dimensions. Indeed, for $N_A(N_B) \geq 3$, we substitute Eq. (13) into Eq. (12), and we can obtain $\Gamma_{\mathbf{V}_M}$. $\Gamma_{\mathbf{V}_M}$ is diagonal, and its diagonal coefficients, which represent the estimation variances of each coefficient of the response matrix, are

$$\mathrm{VAR}[M]^{\mathrm{gau}} = \frac{16}{N_A N_B} \sigma^2 \begin{pmatrix} 1 & 2 & 2 \\ 2 & 4 & 4 \\ 2 & 4 & 4 \end{pmatrix}. \tag{14}$$

For the readout noise of a CCD sensor, it is easily seen in Eq. (14) that the estimation variances for the linear Stokes parameters increase linearly with $1/N_A N_B$. In other words, the estimation precision increases with the number of measurements. It is easy to understand that the larger the number of measurements, the larger the amount of redundant data available to reduce the estimation variance [22,24,25]. If the variance of the noise is proportional to the measurement time, the variance of the matrix is independent of the number of measurements $N_A N_B$.

Next, our goal is to investigate the influence of the incident polarization states and explore the configurations that minimize the impact of incident polarization states on the linear polarization calibration in the presence of Gaussian noise. The configurations are minimized and equalized for $N_A(N_B) \geq 3$ with Gaussian noise. However, the elements of the matrix change substantially if the incident light is polarized partially especially for the configuration of $N_A = 3$, $N_B = 3$. It is easily obtained by using Eq. (6) for different incident Stokes parameters S_1 and S_2 as follows:

$$N_A = 3: \quad G_{A_S} = \frac{3}{4}\begin{pmatrix} 1+\frac{1}{2}S_1^2+\frac{1}{2}S_2^2 & \frac{1}{4}S_1^2-\frac{1}{4}S_2^2+S_1 & S_2-\frac{1}{2}S_1S_2 \\ \frac{1}{4}S_1^2-\frac{1}{4}S_2^2+S_1 & \frac{1}{2}+\frac{3}{8}S_1^2+\frac{1}{8}S_2^2+\frac{1}{2}S_1 & \frac{1}{4}S_1S_2-\frac{1}{2}S_2 \\ S_2-\frac{1}{2}S_1S_2 & \frac{1}{4}S_1S_2-\frac{1}{2}S_2 & \frac{1}{2}+\frac{1}{8}S_1^2+\frac{3}{8}S_2^2-\frac{1}{2}S_1 \end{pmatrix}, \tag{15}$$

$$N_A = 4: \; G_{A_S} = \begin{pmatrix} 1+\frac{1}{2}S_1^2+\frac{1}{2}S_2^2 & S_1 & S_2 \\ S_1 & \frac{1}{2}(1+S_1^2) & 0 \\ S_2 & 0 & \frac{1}{2}(1+S_2^2) \end{pmatrix}, \tag{16}$$

$$N_A \geq 5: \quad G_{A_S} = \frac{N_A}{4} \times \begin{pmatrix} 1+\frac{1}{2}S_1^2+\frac{1}{2}S_2^2 & S_1 & S_2 \\ S_1 & \frac{1}{2}+\frac{3}{8}S_1^2+\frac{1}{8}S_2^2 & 0 \\ S_2 & 0 & \frac{1}{2}+\frac{1}{8}S_1^2+\frac{3}{8}S_2^2 \end{pmatrix}. \tag{17}$$

The following relations have been used to derive Eqs. (15)–(17):

$$\sum_{n=1}^{N_A}\cos 2\theta_i = \sum_{i=1}^{N_A}\sin 2\theta_i = \sum_{i=1}^{N_A}\sin 2\theta_i\cos 2\theta_i = 0,$$
$$\sum_{i=1}^{N_A}\cos^2 2\theta_i = \sum_{i=1}^{N_A}\sin^2 2\theta_i = \frac{N_A}{2}, \tag{18}$$

and

$$N_A = 3: \quad \sum_{i=1}^{N_A}\cos^3 2\theta_i \sin 2\theta_i = \sum_{i=1}^{N_A}\cos 2\theta_i \sin^3 2\theta_i = 0,$$
$$N_A = 4: \quad \sum_{i=1}^{N_A}\cos^4 2\theta_i = \sum_{i=1}^{N_A}\sin^4 2\theta_i = 2, \sum_{i=1}^{N_A}\cos^2 2\theta_i \sin^2 2\theta_i = 0,$$
$$N_A \geq 5: \quad \sum_{i=1}^{N_A}\cos^4 2\theta_i = \sum_{i=1}^{N_A}\sin^4 2\theta_i = \frac{3N_A}{8}, \quad \sum_{i=1}^{N_A}\cos^2 2\theta_i \sin^2 2\theta_i = \frac{N_A}{8}. \tag{19}$$

The covariance matrix $\Gamma_{\mathbf{v}_M}$ for different polarization states is obtained by substituting Eqs. (13) and (15)–(17) in Eq. (12),

$$\mathrm{VAR}[M]_{\mathrm{gau}} = \frac{16}{N_A N_B}\sigma^2 \begin{pmatrix} VM_{g1} & VM_{g2} & VM_{g3} \\ 2VM_{g1} & 2VM_{g2} & 2VM_{g3} \\ 2VM_{g1} & 2VM_{g2} & 2VM_{g3} \end{pmatrix}. \tag{20}$$

The elements are as follows:

$N_A = 3$, $N_B \geq 3$:

$$\begin{cases} VM_{g1} \approx 2/[2-3(S_1^2+S_2^2)] \\ VM_{g2} \approx [3(S_1^2-S_2^2)-4S_1+4]/[(2-3(S_1^2+S_2^2)] \\ VM_{g3} \approx (4+2S_1^2+3S_2^2-4S_1)/[3(S_1^2-S_2^2)-4S_1+2] \end{cases}, \tag{21}$$

$N_A = 4$, $N_B \geq 3$:

$$\begin{cases} VM_{g1} \approx 2(S_1^2+S_2^2+1)/[2-(S_1^2+S_2^2)] \\ VM_{g2} \approx 2(S_1^2-S_2^2+2)/[2-(S_1^2+S_2^2)] \\ VM_{g3} \approx 2(S_2^2-S_1^2+2)/[2-(S_1^2+S_2^2)] \end{cases}, \tag{22}$$

$N_A \geq 5$, $N_B \geq 3$:

$$\begin{cases} VM_{g1} \approx 2(S_1^2+S_2^2+1)/[2-(S_1^2+S_2^2)] \\ VM_{g2} \approx [3(S_1^2-S_2^2)+4]/[2-(S_1^2+S_2^2)] \\ VM_{g3} \approx [2(S_2^2-S_1^2)+1)]/[2-(S_1^2+S_2^2)] \end{cases}. \tag{23}$$

The variance matrix only includes the value that is below the third power of $S_1(S_2)$ or its product due to the DoLP of incident light <0.1 in practice. The difference between approximate calculation and theoretical variance is less than 2‰ of theoretical value, which proves the validity of derivation of Eqs. (21)–(23).

According to Eq. (20), the variances on the second and third rows are twice that on the first row, and the incident Stokes parameters S_1 and S_2 have the same proportion on influence for the same column. For the configurations of $N_A = 3$, $N_B \geq 3$, the estimation variances of different incident polarization states are normalized by the variance matrix coefficient $16\sigma^2/(N_A N_B)$ shown in Fig. 1. For the first column of variance matrix, the variance always increases with S_1 and S_2 from Eq. (21). In contrast, the estimation variance on the second and

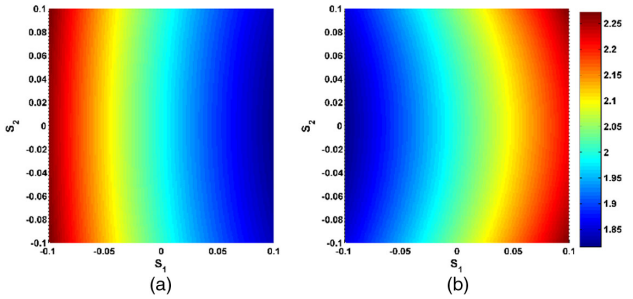

Fig. 1. Estimation variance on (a) the second column VM_{g2} and (b) the third column VM_{g3} for the configuration of $N_A = 3$, $N_B \geq 3$ in the presence of Gaussian noise. $S_1 \in [-0.1, +0.1]$ and $S_2 \in [-0.1, +0.1]$ are considered. Both variance maps are on the same color bar.

third columns depend on the sign of S_1. With the increase of S_1, the variances on the second column are decreased as in Fig. 1(a), and those on the third column are increased as in Fig. 1(b). On the contrary, the variances on the second column are decreased while those on the third column are increased with the increase of absolute S_2.

The estimation variances are normalized by the variance matrix coefficient $16\sigma^2/(N_A N_B)$ for the configurations of $N_A = 4$, $N_B \geq 3$ (top row) and $N_A \geq 5$, $N_B \geq 3$ (bottom row) shown in Fig. 2. It can be easily seen that the variances on the first column increase with S_1 and S_2 from Eqs. (22) and (23). The configurations of $N_A = 4$, $N_B \geq 3$ have no cross talk. In other words, S_1 only influences the variances on second column in Fig. 2(a) while S_2 only influences the third column in Fig. 2(b). Moreover, the variances on the second/third column are increased with the absolute value of S_1/S_2. In contrast, for the configurations of $N_A = 5$, $N_B \geq 3$, S_1 and S_2 have influence on all elements of variance matrix as in Figs. 2(c) and 2(d).

C. Poisson Noise

Let us consider that the measurements are corrupted by Poisson noise. We use property of Poisson noise that its variance is equal to its mean value, and the diagonal of the covariance matrix $\Gamma_{\mathbf{V}_I}$ as [20]

$$\forall n \in [1,\ N_A N_B], \quad (\Gamma_{V_I})_{nn} = \langle V_I \rangle = \sum_{i=1}^{16} [B \otimes A_S]_{ni} [V_M]_i. \tag{24}$$

It is easy to rewrite the diagonal element of the matrix $\Gamma_{\mathbf{V}_M}$ by substituting Eq. (24) in Eq. (11),

$$(\Gamma_{\mathbf{V}_M})_{ii} = \sum_{j=1}^{16} Q_{ij} [\mathbf{V}_M]_j, \tag{25}$$

where Q is a 9×9 matrix having the following expression as [20]

$$Q_{ij} = \sum_{n=1}^{N_A N_B} (P_{in})^2 [B \otimes A_S]_{nj}. \tag{26}$$

It can be seen that Q represents the influence of the element $M_{11} - M_{33}$ of response matrix on variance matrix, and column of Q is the variance value of $M_{11} - M_{33}$. If the Stokes vector of incident light is [1;0;0], after cumbersome, but elementary, computations, one obtains the following expressions of the covariance matrix that depend on the numbers of measurements N_A, N_B by substituting Eqs. (6) and (13) into Eq. (25):

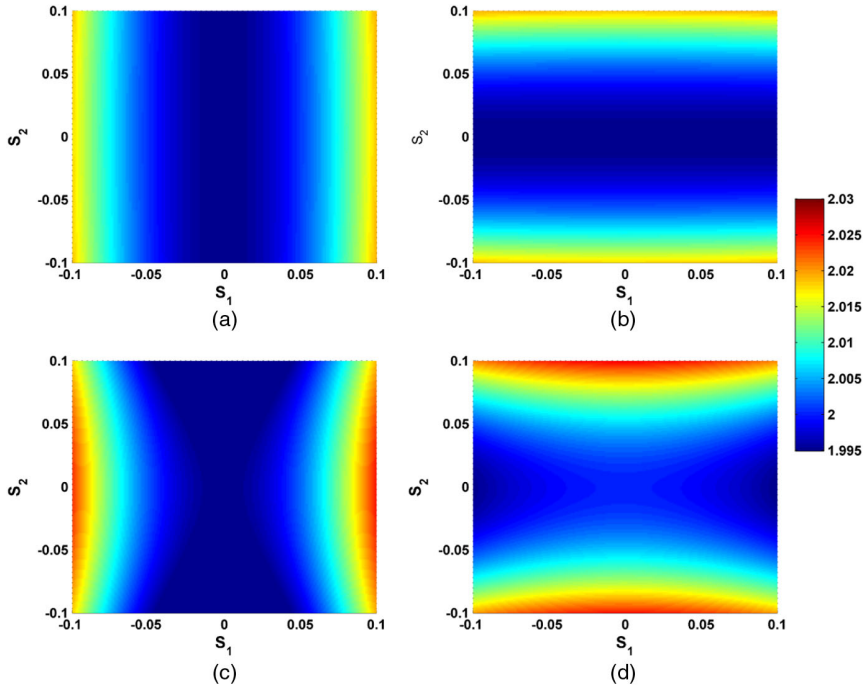

Fig. 2. Estimation variance for the configuration of $N_A = 4$, $N_B \geq 3$ on (a) the second column VM_{g2}, (b) the third column VM_{g3}, and that for the configuration of $N_A \geq 5$, $N_B \geq 3$ on (c) the second column VM_{g2}, (d) the third column VM_{g3} in the presence of Gaussian noise. $S_1 \in [-0.1, +0.1]$ and $S_2 \in [-0.1, +0.1]$ are considered. All variance maps are on the same color bar.

$$N_A=3,\ N_B=3:\quad \mathrm{VAR}[M]^{\mathrm{poi}}=\frac{4}{9}I_0\left(M_{11}\begin{pmatrix}1&2&2\\2&4&4\\2&4&4\end{pmatrix}+M_{12}\begin{pmatrix}0&1&-1\\0&2&-2\\0&2&-2\end{pmatrix}+M_{21}\begin{pmatrix}0&0&0\\1&2&2\\-1&-2&-2\end{pmatrix}+M_{22}\begin{pmatrix}0&0&0\\0&1&-1\\0&-1&1\end{pmatrix}\right),\tag{27}$$

$$N_A\geq 4,\ N_B=3:\quad \mathrm{VAR}[M]^{\mathrm{poi}}=\frac{4}{3N_A}I_0\left(M_{11}\begin{pmatrix}1&2&2\\2&4&4\\2&4&4\end{pmatrix}+M_{21}\begin{pmatrix}0&0&0\\1&2&2\\-1&-2&-2\end{pmatrix}\right),\tag{28}$$

$$N_A\geq 4,\ N_B\geq 4:\quad \mathrm{VAR}[M]^{\mathrm{poi}}=\frac{4I_0M_{11}}{N_AN_B}\begin{pmatrix}1&2&2\\2&4&4\\2&4&4\end{pmatrix}.\tag{29}$$

M_{ij} represents the value of the response matrix seen in Eq. (1). It is easily seen from Eqs. (27)–(29) that the variances depend on the reflectivity of optical system. The configuration of $N_A=3$, $N_B=3$ has four terms of response matrix M_{11}, M_{12}, M_{21}, and M_{22} from Eq. (27). Obviously, M_{22} seriously influences on the estimation precision because the diagonal element of the response matrix is approximately 1 or −1. In contrast, the configurations of $N_A\geq 4$, $N_B=3$ have two terms M_{11}, M_{21} from Eq. (28), which means that these configurations are less susceptible to the elements of response matrix compared with the configuration of $N_A=3$, $N_B=3$. The variances only depend on the measured response matrix only through its intensity reflectivity M_{11} term for configurations of $N_A\geq 4$, $N_B\geq 4$ from Eq. (29). Compared with the configurations of $N_A\geq 4$, $N_B\geq 4$, the configuration of $N_A\geq 4$, $N_B=3$ must ensure M_{21} close to 0, which can minimize and equalize the estimation variances. For an instrument based on three polarizers oriented at 0°, 60°, 120°, it must be noted that the optical system is optimized as much as possible to reduce the impact of M_{21}.

Next, let us consider that $\Gamma_{\mathbf{v}_M}$ is influenced by different incident Stokes parameters S_1 and S_2. M_{11} and M_{22} terms close to 1 have large influence on estimation variance in practice. In contrast, M_{12}, M_{21} terms are close to zero, and the influences of them are far less than M_{11}, M_{22} terms. Therefore, we only investigate the variation of variance matrix of M_{11}, M_{22} terms for different incident polarization states. The variance matrix only includes the value that is below the third power of $S_1(S_2)$ or its product. It can be rewritten by substituting Eqs. (15)–(17) in Eq. (25) as

$$\mathrm{VAR}[M]_{\mathrm{poi}}=\frac{4IM_{11}}{N_AN_B}\begin{pmatrix}VM_{p1}&VM_{p2}&VM_{p3}\\2VM_{p1}&2VM_{p2}&2VM_{p3}\\2VM_{p1}&2VM_{p2}&2VM_{p3}\end{pmatrix}+\frac{4IM_{22}}{N_AN_B}\begin{pmatrix}0&0&0\\VM_{p4}&VM_{p5}&VM_{p6}\\-VM_{p4}&-VM_{p5}&-VM_{p6}\end{pmatrix},\tag{30}$$

and the elements are as follows:

$N_A=3,\ N_B\geq 3$:

$$\begin{cases}VM_{p1}\approx 2(1-S_1-S_2^2)/(2-2S_1-S_1^2-3S_2^2)\\VM_{p2}\approx(4-6S_1+3S_1^2-5S_2^2)/(2-2S_1-S_1^2-3S_2^2)\\VM_{p3}\approx(4-6S_1+3S_1^2-3S_2^2)/(2-4S_1+3S_1^2-3S_2^2)\end{cases},\tag{31}$$

and if

$$N_A=3,\ N_B=3:\quad \begin{cases}VM_{p4}\approx(2S_1+S_2^2-S_1^2)/(-4+12S_1^2+12S_2^2)\\VM_{p5}\approx(6S_1+7S_1^2+13S_2^2-4)/(-4+12S_1^2+12S_2^2)\\VM_{p6}\approx(-14S_1+6S_1^2-9S_2^2+4)/(4-16S_1+28S_1^2-12S_2^2)\end{cases},\tag{32}$$

and if $N_A=3$, $N_B>3$, the elements $(VM_{p4}, VM_{p5}, VM_{p6})$ of variance matrix of M_{22} are equal to zero,

$$N_A\geq 4,\ N_B\geq 3:\quad \begin{cases}VM_{p1}\approx 2/(2-S_1^2-S_2^2)\\VM_{p2}\approx(1-S_2^2)/(1-S_1^2-S_2^2)\\VM_{p3}\approx(1-S_1^2)/(1-S_1^2-S_2^2)\end{cases},\tag{33}$$

and if

$$N_A=4,\ N_B=3:\quad \begin{cases}VM_{p4}\approx S_1/2\\VM_{p5}\approx -2S_1\\VM_{p6}\approx 0\end{cases},\tag{34}$$

and if

$N_A>4,\ N_B=3$:

$$\begin{cases}VM_{p4}\approx(2S_1+S_1^2-S_2^2)/[4(1-S_1^2-S_2^2)]\\VM_{p5}\approx -S_1/[2(1+S_1^2-S_2^2)]\\VM_{p6}\approx[3(2S_1+S_2^2-S_1^2)]/[4(1+S_1^2-S_2^2)]\end{cases},\tag{35}$$

and if $N_A\geq 4$, $N_B\geq 4$, the elements $(VM_{p4}, VM_{p5}, VM_{p6})$ of variance matrix of M_{22} are equal to zero. We also have used the relations of Eqs. (18) and (19) to derive Eqs. (30)–(35). The difference for the variance matrix of M_{11} term between approximate calculation and theoretical results is less than 3.0‰ of

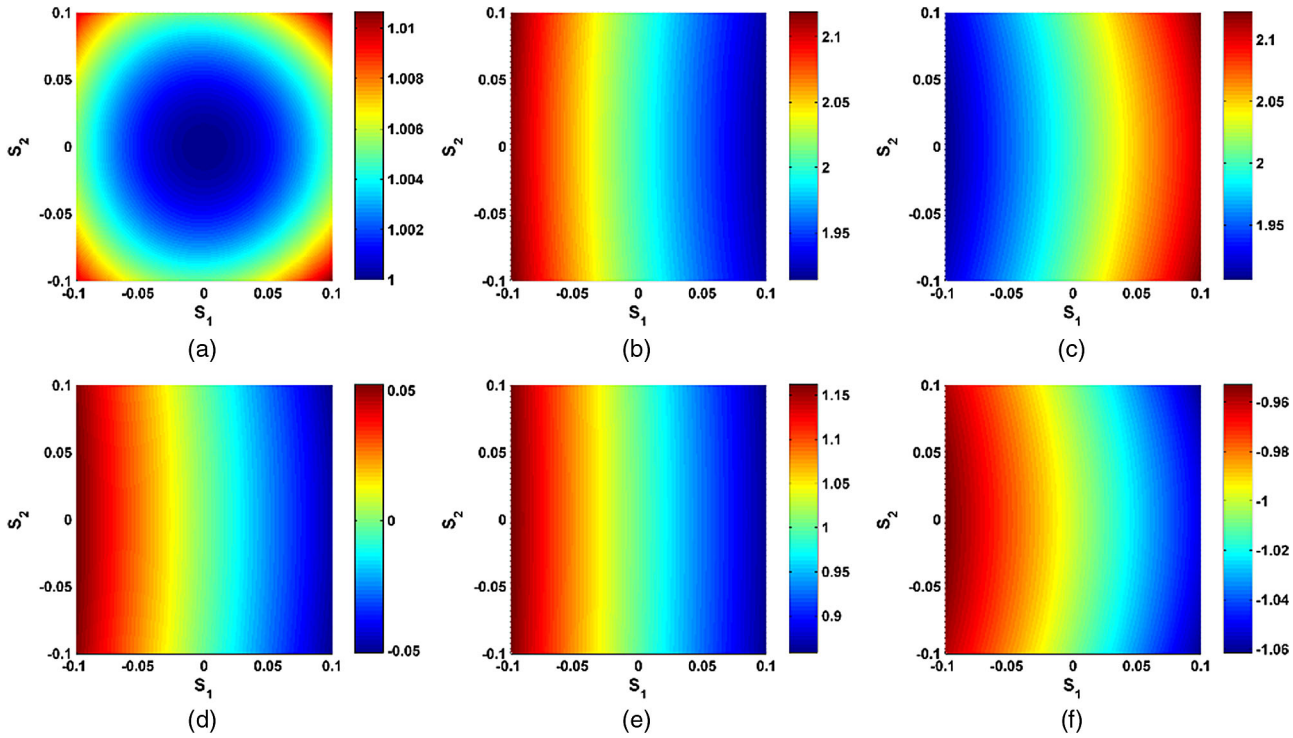

Fig. 3. Estimation variance of the configuration of $N_A = 3$, $N_B = 3$ with (a) VM_{p1}, (b) VM_{p2}, (c) VM_{p3} for M_{11} term and (d) VM_{p4}, (e) VM_{p5}, (f) VM_{p6} for M_{22} term in the presence of Poisson noise. $S_1 \in [-0.1, +0.1]$ and $S_2 \in [-0.1, +0.1]$ are considered.

theoretical value for the configurations of $N_A \geq 3$, $N_B N_A \geq 3$, and the difference for M_{22} is less than 4.0‰ except 2.2% for VM_{p4} of the configurations of $N_A \geq 4$, $N_B = 3$. Therefore, Eqs. (31)–(35) are valid if $S_1, S_2 \in [-0.1, 0.1]$.

The estimation variances of M_{11} and M_{22} terms for different incident polarization states in the presence of Poisson noise are normalized by the variance matrix coefficient $4IM_{11}/N_A N_B$ and $4IM_{22}/N_A N_B$ shown in Fig. 3. For the configuration of $N_A = 3$, $N_B = 3$, the variances of M_{11} terms on the first column are increased with absolute S_1 and S_2 as in Fig. 3(a) while the variances on the second and third column have similar but less influence with those on the second and third column for Gaussian noise at the same configuration shown in Figs. 3(b) and 3(c). Considering the variance matrix of M_{22} term, the elements VM_{P4}, VM_{P5}, and VM_{P6} are decreased with the increase of S_1 and absolute S_2 shown in Figs. 3(d)–3(f). It must be noted that the variation trends are opposite for the variance between the second row and the third row due to the negative sign of the third row from Eq. (30).

In contrast, all variances of M_{11} term are increased with absolute S_1 and absolute S_2 for the configuration of $N_A = 4$, $N_B = 3$ as in Figs. 4(a)–4(c). It is clear that, for VM_{P4} or VM_{P5} of M_{22} term, the variance increases linearly with $S_1/2$ or $-2S_1$ from Eq. (34), as shown in Figs. 4(d) and 4(e). According to Eqs. (34) and (35), for the configuration of $N_A > 4$, $N_B = 3$, the Stokes parameters S_1 and S_2 have less influence on variance matrix of M_{22} terms compared with the configuration of $N_A = 4$, $N_B = 3$. One must be cautious to select the configuration of $N_A \geq 4$, $N_B = 3$, and the precision of this configuration is susceptible to incident polarization states due to the variance matrix of M_{22} term. Moreover, the variations on variance for the configuration of $N_A \geq 4$, $N_B \geq 4$ are small because they are only influenced by M_{11} compared with other configurations shown by Eq. (33). When we superpose variance matrix of M_{11} and M_{22} terms, the total variance matrix will be obtained. We will illustrate this point in the simulations.

For the configuration of $N_A = 4$, $N_B = 3$, if the Stokes parameters S_1 and S_2 of incident light are approximately equal to 0, the incident light has less influence on estimation variance matrix, but we need to consider the influence of M_{21} terms seen Eq. (28). However, with the increase of Stokes parameters S_1 and S_2 of incident light, the variations due to incident polarization states on estimation variance are generally increased, and the influence of incident polarization states for configuration of $N_A > 4$, $N_B = 3$ is less than the one for configuration of $N_A = 4$, $N_B = 3$. Moreover, different polarization states cannot influence the estimation variance matrix of M_{22} term for configuration of $N_A \geq 4$, $N_B \geq 4$. Combined with the above analysis, we can come to the following conclusion: the configurations of $N_A \geq 4$, $N_B \geq 4$ are optimal to minimize the influences of incident light and only depend on the reflectivity of the material.

3. MONTE CARLO SIMULATIONS

During Monte Carlo simulations, we assume that the response matrix has the form of $M = \mathrm{diag}(1, 1, 1)$. This matrix is also widely used in theoretical calculations, and the variance matrix for the configuration of $N_A = 3$, $N_B = 3$ is obtained as

$$\mathrm{VAR}[M]^{\mathrm{poi}} = \frac{4}{9} I_0 \begin{pmatrix} 1 & 2 & 2 \\ 2 & 5 & 3 \\ 2 & 3 & 5 \end{pmatrix}. \tag{36}$$

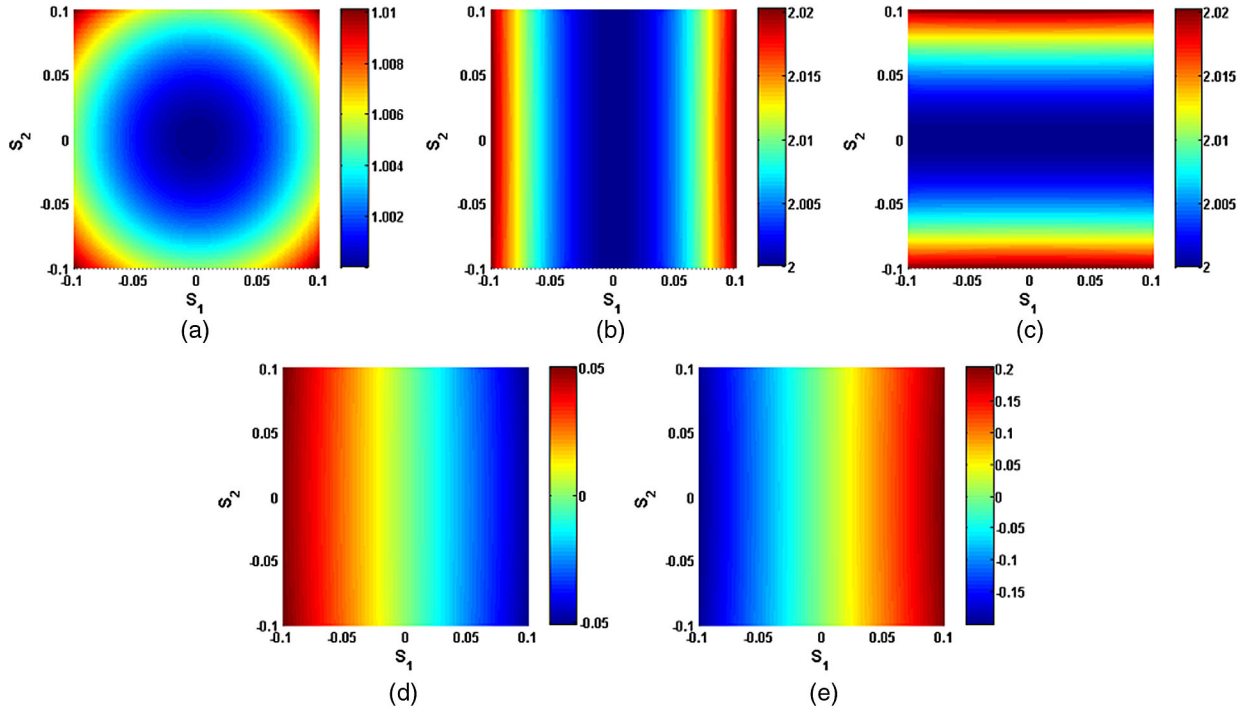

Fig. 4. Estimation variance of the configuration of $N_A = 4$, $N_B = 3$ with (a) VM_{p1}, (b) VM_{p2}, (c) VM_{p3} for M_{11} term and (d) VM_{p4}, (e) VM_{p5} for M_{22} term in the presence of Poisson noise. $S_1 \in [-0.1, +0.1]$ and $S_2 \in [-0.1, +0.1]$ are considered.

This configuration is important to determine the types of noise due to the difference between Gaussian and Poisson noise on variance matrix. In the simulations, we assume that there are no measurement errors, but that the intensities are only influenced by Gaussian or Poisson noise with different incident polarization states. In the actual environment, the matrix deviates from the ideal case due to the systematic errors and other types of noise. This point will be discussed further in the next section.

To obtain the influence of incident polarization states, $[1; -0.1; 0]$ is employed to estimate the precision of the response matrix for linear polarization calibration. Three configurations are used to compare the influences of the numbers of the PSGs and PSAs. The first configuration is $N_A = 3$, $N_B = 3$, which is sensitive to the incident polarization states. The second configuration is $N_A = 4$, $N_B = 3$, which is to analyze the influence on the variance matrix of M_{22} term. The third configuration is $N_A = 4$, $N_B = 4$, and it is less susceptible to partial polarized incident light.

We assume variance matrices $VAR[M]$ in the presence of Gaussian noise with a zero-mean and $\sigma^2 = 1$, and in the presence of Poisson noise that its variance is equal to its mean value. The results from Monte Carlo simulations are shown in Table 1. It is easy to find that the results are in a good agreement with theoretical values obtained from 10^6 random realizations. The differences between the simulated and theoretical values are less than 1.1% with Stokes vector $[1; -0.1; 0]$ and 2.0% with $[1; 0; 0]$ for each element.

Three configurations are close to that predicted by theory with unpolarized incident light from Eqs. (14) and (27)–(29). The simulated and theoretical results are normalized by $16\sigma^2/(N_A N_B)$ for Gaussian noise and $4IM_{11}/(N_A N_B)$ for Poisson noise illustrated in Fig. 5.

Let us now analyze the configuration of $N_A = 3$, $N_B = 3$ in the presence of Gaussian noise. It can be easily seen that the amplitudes of variation of first column are less than 2.5% of their value with unpolarized incident light. The second column is increased 11.7% while the third column is decreased 9.6%. For Poisson noise, with Stokes vector $[1; -0.1; 0]$, the variance VM_{P2} of the second column of M_{11} term is grown to 2.12, and the variance VM_{P5} is 1.16 shown in Fig. 3. When we superpose them, we can obtain the variance of M_{22} that $2VM_{P2} + VM_{P5} = 5.40$. That is similar with the simulation result and is increased 8%. The variance of M_{32} is increased 3.7% due to the opposite sign between the second and third row of variance matrix for M_{22} term from Eq. (30). The variances of M_{13}, M_{23}, and M_{33} are decreased 5.5%, 7.0% and 5.0%, respectively.

Next, let us now analyze the configuration of $N_A = 4$, $N_B = 3$ in the presence of Gaussian noise. The amplitudes of variation of all elements are less than 2.1% of their value with unpolarized incident light, which means that the configuration of $N_A = 4$, $N_B = 3$ is insensitive to incident polarization states for Gaussian noise. However, the variance of M_{21} is increased 4% while the one of M_{31} is decreased 1%; in addition, the decrease of 3.5% and the increase of 4.8% are obtained for the variations of M_{22} and M_{32} due to the variance matrix of M_{22} term from Eqs. (30) and (34).

For the configuration of 4×4, the amplitudes of variation of all the elements for the variance matrix are less 2% in the presence of Gaussian and Poisson noise. Obviously, the

Table 1. Results of Variance Matrix for Three Forms That $N_A \times N_B$ Is Equal to 3 × 3, 4 × 3, and 4 × 4 for Two Types of Incident Light ([1; 0; 0] and [1; −0. 1; 0]) in Linear Polarization Calibration

$N_A \times N_B$	$\mathrm{VAR}[M]^{Gau} = 16\sigma^2/(N_A N_B)\times$		$\mathrm{VAR}[M]^{Poi} = 4I/(N_A N_B)\times$	
	$S_1 = 0$	$S_1 = -0.1$	$S_1 = 0$	$S_1 = -0.1$
3 × 3	$\begin{pmatrix} 1.00 & 2.01 & 2.00 \\ 1.95 & 4.01 & 4.00 \\ 2.00 & 4.01 & 4.00 \end{pmatrix}$	$\begin{pmatrix} 1.00 & 2.19 & 1.82 \\ 2.00 & 4.37 & 3.63 \\ 1.99 & 4.42 & 3.59 \end{pmatrix}$	$\begin{pmatrix} 1.00 & 1.99 & 1.98 \\ 1.97 & 4.96 & 3.00 \\ 1.99 & 2.97 & 4.92 \end{pmatrix}$	$\begin{pmatrix} 1.00 & 2.17 & 1.89 \\ 2.09 & 5.43 & 2.79 \\ 1.93 & 3.11 & 4.75 \end{pmatrix}$
4 × 3	$\begin{pmatrix} 1.00 & 1.99 & 2.03 \\ 1.99 & 3.98 & 4.00 \\ 2.00 & 3.99 & 3.97 \end{pmatrix}$	$1.02\begin{pmatrix} 1.00 & 2.03 & 1.99 \\ 2.02 & 3.99 & 3.98 \\ 2.03 & 4.01 & 3.94 \end{pmatrix}$	$\begin{pmatrix} 1.00 & 2.00 & 1.97 \\ 2.00 & 3.99 & 3.99 \\ 1.96 & 3.97 & 4.01 \end{pmatrix}$	$1.01\begin{pmatrix} 1.00 & 2.01 & 1.99 \\ 2.00 & 3.82 & 4.01 \\ 1.98 & 4.15 & 3.98 \end{pmatrix}$
4 × 4	$\begin{pmatrix} 1.01 & 1.99 & 1.99 \\ 2.01 & 4.01 & 3.99 \\ 1.99 & 4.02 & 4.00 \end{pmatrix}$	$1.01\begin{pmatrix} 1.00 & 1.98 & 1.99 \\ 2.02 & 4.01 & 4.00 \\ 2.01 & 3.97 & 4.01 \end{pmatrix}$	$\begin{pmatrix} 1.00 & 2.01 & 1.98 \\ 1.96 & 4.01 & 4.00 \\ 1.99 & 3.98 & 3.99 \end{pmatrix}$	$1.01\begin{pmatrix} 1.00 & 2.01 & 2.00 \\ 2.03 & 3.98 & 4.01 \\ 1.99 & 3.99 & 4.01 \end{pmatrix}$

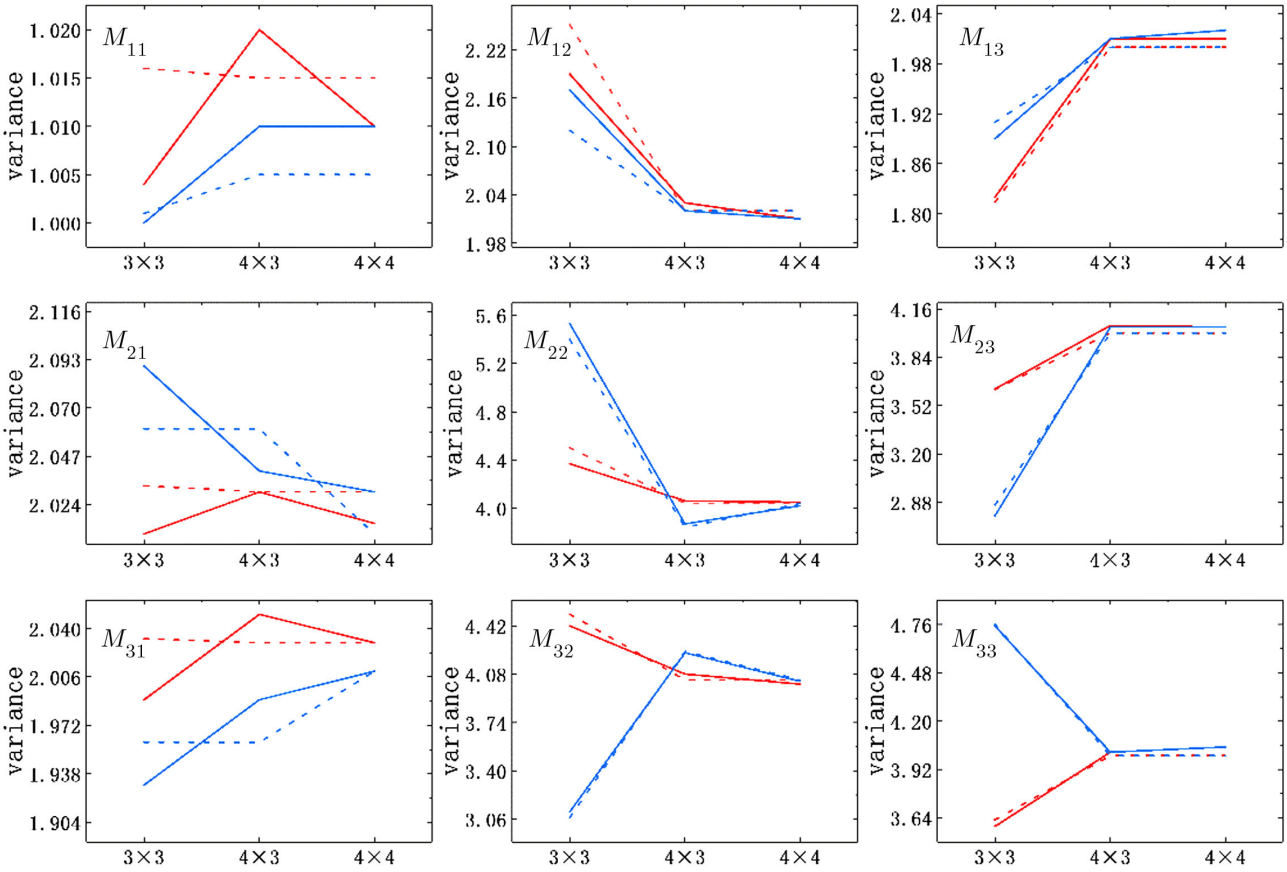

Fig. 5. Simulated and theoretical results for the configuration of 3 × 3, 4 × 3, and 4 × 4 with Stokes vector [1; −0.1; 0]. They are normalized by $16\sigma^2/(N_A N_B)$ for Gaussian noise and $4I/(N_A N_B)$ for Poisson noise. Solid lines show the simulation results, and dashed lines show the theoretical results. Colors are used for different sets of noise: Gaussian noise (red); Poisson noise (blue).

configuration of 4 × 4 is more suitable for partial polarized light, which is consistent with the analysis of theory.

4. EXPERIMENTS

A. Experimental Setups

The PSG and PSA have the same component, and both are composed of a polarizer (CODIXX, COLORPOL-VIS-600-BC5). One of them can be rotated by 360° via a motorized rotation stage (Zolix, RAK100), and another one is rotated by a manual rotation stage (Zolix, KSMR5A-120). The light beam emitted from an integrating sphere passes through two polarizers. A spike filter was used at 700 nm; the extinction ratio of the polarizer at this wavelength is less than 1:100,000. The intensity fluctuations were checked to be negligible (approximately <0.5% in half an hour).

The experimental setup is shown in Fig. 6. First, no component between the PSG and the PSA is used to study the influence of incident polarization states, and two collimators are employed to produce two types of incident polarization states.

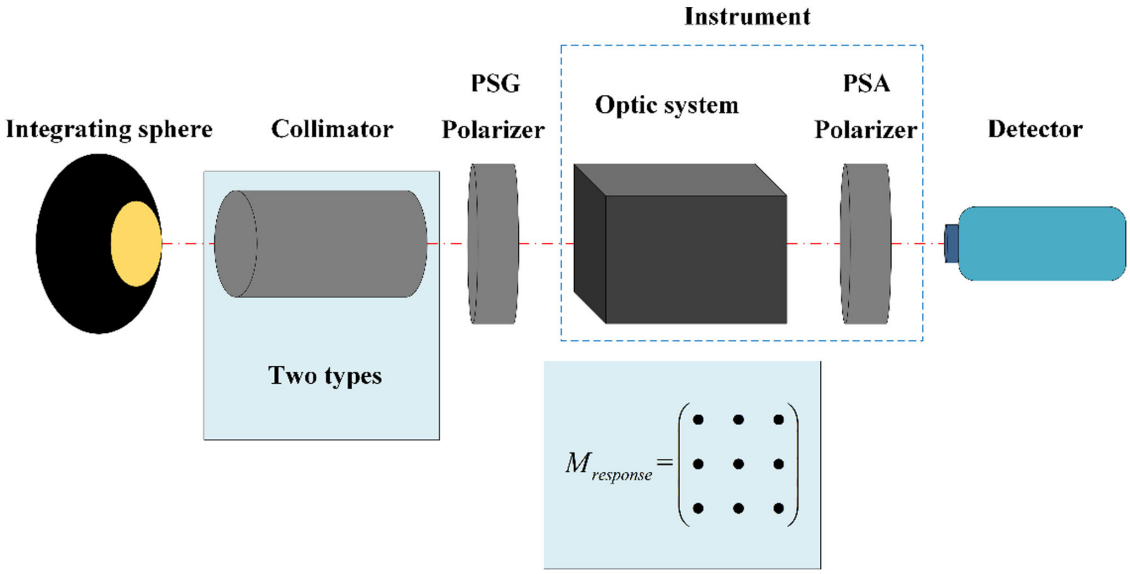

Fig. 6. Optical schema for the verification of the calibration strategy.

Table 2. Experimental Results for Different N_A and N_B[a]

	A1	A2	A3
$\mathrm{VAR[M]}_{3\times3} = I_{1-3}\times$	$\begin{pmatrix} 1.00 & 1.82 & 1.97 \\ 1.83 & 4.96 & 2.91 \\ 1.89 & 2.98 & 4.84 \end{pmatrix}$	$\begin{pmatrix} 1.00 & 1.97 & 1.82 \\ 1.93 & 5.20 & 2.81 \\ 1.90 & 3.06 & 4.81 \end{pmatrix}$	$\begin{pmatrix} 1.00 & 1.89 & 2.01 \\ 1.84 & 4.97 & 2.91 \\ 1.87 & 2.89 & 4.84 \end{pmatrix}$
I_{1-3}	115	117	95
$\mathrm{VAR[M]}_{4\times3} = I_{4-6}\times$	$\begin{pmatrix} 1.00 & 2.03 & 1.98 \\ 2.04 & 3.96 & 4.02 \\ 1.94 & 4.03 & 3.93 \end{pmatrix}$	$\begin{pmatrix} 1.00 & 2.02 & 1.99 \\ 2.08 & 3.88 & 4.08 \\ 1.98 & 4.13 & 3.99 \end{pmatrix}$	$\begin{pmatrix} 1.00 & 2.00 & 1.99 \\ 1.99 & 3.98 & 4.10 \\ 2.01 & 4.01 & 3.86 \end{pmatrix}$
I_{4-6}	71	73	68
$\mathrm{VAR[M]}_{5\times5} = I_{7-9}\times$	$\begin{pmatrix} 1.00 & 1.97 & 2.00 \\ 2.02 & 3.97 & 4.09 \\ 2.00 & 4.05 & 3.92 \end{pmatrix}$	$\begin{pmatrix} 1.00 & 2.00 & 1.99 \\ 2.04 & 4.04 & 4.11 \\ 1.97 & 3.96 & 3.89 \end{pmatrix}$	$\begin{pmatrix} 1.00 & 2.00 & 1.98 \\ 1.98 & 3.92 & 3.99 \\ 2.01 & 4.04 & 3.93 \end{pmatrix}$
I_{7-9}	35	35	32

[a]A1 employs one collimator to produce the low-level DoLP (about 2.5%) ($S_1 = -0.02$, $S_2 = -0.01$), and A2 employs another collimator with the DoLP (about 8.9%) ($S_1 = -0.04$, $S_2 = -0.08$); A3 consists of a telescopic system with the incident light of low-level DoLP ($S_1 = -0.02$, $S_2 = -0.01$).

Second, the response matrix consists of a telescopic system to provide the comparison of the real response matrix. Every experiment employs $N_A \times N_B = (3\times3, 4\times3, 5\times5)$. The estimation variance is easily influenced by the incident light for the configuration of 3×3, which is the key to verifying the validity of the theory. The configuration of 4×3 is used to figure out whether or not the optical system (M_{21} and M_{22}) has an impact on the estimation variance, and the configuration of 5×5 used to provide an optimal reference is one of the optimal configurations. A CMOS camera (Ximea, MQ042CG-CM) with 100×100 pixels is employed to calculate the variance. The experiments were carried out under multiple conditions to verify the theory according to the steps above.

B. Discussion

The matrices for the estimation variance are described in Table 2. It can be easily seen that the dominant noise is Poisson noise according to Eqs. (14) and (36). The trend of experimental and theoretical results for the configurations of 3×3, 4×3, and 5×5 is consistent and illuminated in Fig. 7. It can be seen that, for the configuration of 3×3, the variances of M_{22} and M_{32} are increased 4.8% and 1.5% in 8.9% DoLP compared with 2.5% DoLP. In contrast, the variances of M_{23} and M_{33} are increased 3.3% and 0.6% in 8.9% DoLP. For the configuration of 4×3, compared with 2.5% DoLP, the variance of M_{22} has the decrease of 2.0%, and the one of M_{32} is increased 2.5% in 8.9% DoLP. Therefore, the configuration of 4×3 is more stable than the one of 3×3. For the configuration of 5×5, the variance matrix with 8.9% DoLP is closer to the one with unpolarized light, which means that this configuration is less susceptible to different incident polarization states. Furthermore, It is easily seen from Eq. (28) that for the configuration of 4×3 the influence of M_{21} term on variance is less than that of M_{11} and M_{22} terms because the difference between A2 and A1 is larger than that between A3 and A1 from the variance matrix on the second row in Fig. 7 (middle row) and the third row Fig. 7 (bottom row).

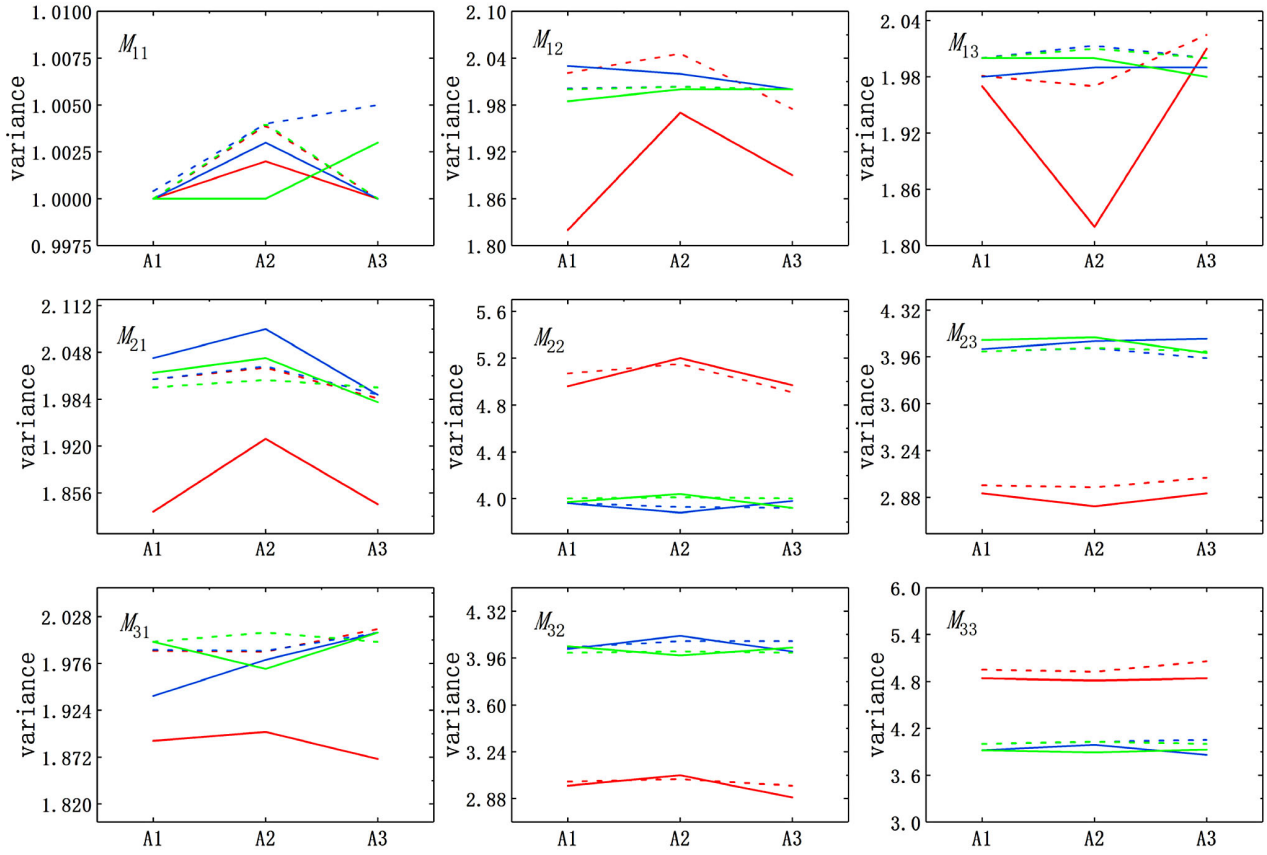

Fig. 7. Normalized simulated and theoretical results for A1 (2.5% DoLP of incident light); A2 (about 8.9% DoLP of incident light); A3 (consisting of telescopic system 2.5% DoLP). Solid lines show the experimental results, and dashed lines show the theoretical results. Colors are used for different sets of configurations: 3 × 3 (red), 4 × 3 (blue), 5 × 5 (green).

The same conclusion has been obtained from theory. After 10 repeated measurements, under the same circumstance, a normalized element precision of 1.3% was ensured. M_{os} represents the response matrix of the optical system in A_3, and M_{no} represents that of no component between the PSG and the PSA in A_1 and A_2,

$$M_{no} = \begin{pmatrix} 1 & 0.001 & 0.001 \\ 0.008 & 0.992 & -0.010 \\ 0.007 & -0.013 & 0.993 \end{pmatrix}, \tag{37}$$

$$M_{os} = \begin{pmatrix} 1 & -0.045 & -0.074 \\ -0.0243 & 0.980 & 0.005 \\ -0.040 & -0.006 & 0.981 \end{pmatrix}. \tag{38}$$

The proposed method for analysis of the influence of different incident polarization states can be used to analyze the types of noise and to choose the minimum numbers of PSGs and PSAs.

C. Systematic Errors

In the derivation of the theory, we only consider the influence of Gaussian and Poisson noise. However, the actual response matrix will deviate from the theory due to other types of noise and errors. The other types of noise are uniform noise, salt and pepper noise, and compound noise, and the errors are rotational error, intensity fluctuation, and alignment errors.

It is difficult to derive an analytical solution, so we add these noise types into the intensities by Monte Carlo simulation to analyze the estimation precision. It is found that the estimation variances are analogous to the case of Gaussian or Poisson noise for the optimal configurations with two types of incident polarization states in simulations, which means that the other types of noise have no significant influence on the element of variance matrix but only to increase or decrease the coefficient of variance matrix, and incident polarization state as an independent variable is valid. The conclusion was verified in the experiments.

Ten repeated measurements were made to obtain the measurement precision for the errors, as shown in Fig. 8. The relative differences over 10 repeated measurements are found to be less than 3.0% for each measurement and 0.7% for the mean of 10 repeated measurements, respectively. It is found that the real variance matrix deviated from the ideal values a little bit, but its trend is still consistent with theory. It is obvious that the variation due to systematic errors and noise 0.7% is less than 3.8% due to the incident polarization state for a configuration of 3 × 3. The variations due to 8.9% DoLP for the configurations of 4 × 3 and 5 × 5 are about 2.1% and 1.0%. That means that small systematic errors and other noise have no significant influence and are less than the influence of 8.9% DoLP in the polarization calibration on the configuration of 3 × 3 and 4 × 3, which can ensure the validity of the experiment.

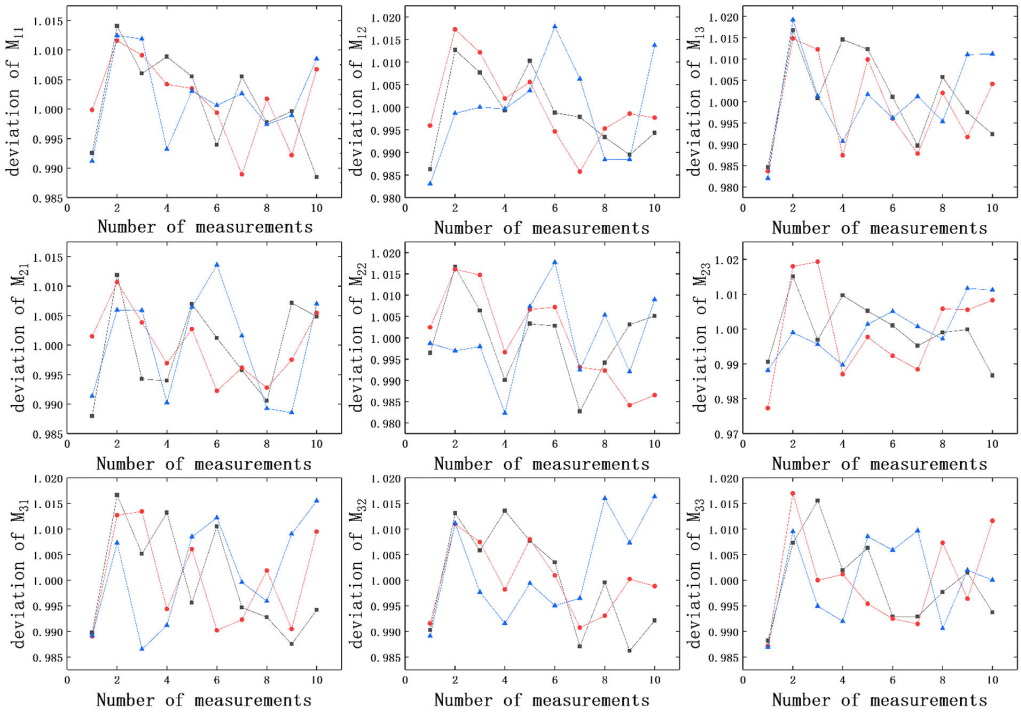

Fig. 8. Deviation of 10 repeated measurements for the configuration of 3×3 (blue), 4×3 (red), and 5×5 (black) on response matrix ($M_{11} - M_{33}$). Each estimation variance is normalized by the mean value of variance for 10 measurements.

5. CONCLUSION

In summary, restricting ourselves to the linear Stokes calibration, we have derived the analytical solution for the estimation variance of the response matrix with partially polarized light, in the presence of Gaussian and Poisson noise. We obtain the optimal configurations of $N_A \geq 3$, $N_B \geq 3$ for Gaussian noise; however, the incident light is found to have a great influence on the configuration of $N_A = 3$, $N_B = 3$. Additionally, a configuration of at least $N_A = 4$, $N_B = 3$ is required to calibrate the instrument for Poisson noise. However, the incident light and response matrix of the optical system except for the reflectivity are found to influence the stability of the estimation variance matrix. By contrast, the configurations of $N_A \geq 4$, $N_B \geq 4$ are optimal for different incident polarization states and two types of noise. The theoretical results are verified with the Monte Carlo simulations and practical experiments. In the experiments, the sets of configurations for $N_A = 3$, $N_B = 3$; $N_A = 4$, $N_B = 3$; and $N_A = 5$, $N_B = 5$ are presented. The experimental results are consistent with the theoretical analysis.

Different calibration methods and configurations have different influences on the estimation variance for different incident polarization states in the presence of two types of noise, and the theory can provide a new approach to obtain the stable estimation variance matrix. This paper analyzes the influence of incident light, which is important for analyzing the precision in the initial design of a polarization imager [26]. We can adopt an effective calibration method to ensure the precision in practice according to different incident polarization states. These results will make it possible to assess extreme precision. Although we investigate the estimation variance in the presence of two types of noise, this method shows good adaptability to other kinds of noise with a certain mean and variance. The normalized precision of the response matrix will be developed in the future.

Funding. CAS Strategic Pioneer Program on Space Science (XDA15320000, XDA15320100, XDA15320103); Joint Fund of Astronomy (U1931118).

Acknowledgment. We thank the x ray and EUV optics technology laboratory in Changchun Institute of Optics and Fine Mechanics and Physics (CIOMP) for supporting this research.

Disclosures. The authors declare no conflicts of interest.

REFERENCES

1. T. G. Moran, J. M. Davila, J. S. Morrill, D. Wang, and R. Howard, "Solar and heliospheric observatory/large angle spectrometric coronagraph polarimetric calibration," Sol. Phys. **237**, 211–222 (2006).
2. R. Howard, J. Moses, A. Vourlidas, J. Newmark, D. Socker, S. Plunkett, C. Korendyke, J. Cook, A. Hurley, and J. Davila, "Sun Earth connection coronal and heliospheric investigation (SECCHI)," Space Sci. Rev. **136**, 67–115 (2008).
3. G. Giono, R. Ishikawa, N. Narukage, R. Kano, Y. Katsukawa, M. Kubo, S. Ishikawa, T. Bando, H. Hara, and Y. Suematsu, "Polarization calibration of the chromospheric Lyman-alpha spectropolarimeter for a 0.1% polarization sensitivity in the VUV range. Part I: pre-flight calibration," Sol. Phys. **291**, 3831–3867 (2016).
4. G. Giono, R. Ishikawa, N. Narukage, R. Kano, Y. Katsukawa, M. Kubo, S.-N. Ishikawa, T. Bando, H. Hara, and Y. Suematsu, "Polarization calibration of the chromospheric Lyman-Alpha spectro polarimeter for a 0.1% polarization sensitivity in the VUV range. Part II: in-flight calibration," Sol. Phys. **292**, 57 (2017).

5. Y. Fu, Z. Huang, H. He, H. Ma, and J. Wu, "Flexible 3 × 3 Mueller matrix endoscope prototype for cancer detection," IEEE Trans. Instrum. Meas. **67**, 1700–1712 (2018).
6. Z. Ding, Y. Yao, X. S. Yao, X. Chen, C. Wang, S. Wang, and T. Liu, "Demonstration of compact in situ Mueller-matrix polarimetry based on binary polarization rotators," IEEE Access **7**, 144561 (2019).
7. J. Yang, T. Du, B. Niu, C. Li, J. Qian, and L. Guo, "A bionic polarization navigation sensor based on polarizing beam splitter," IEEE Access **6**, 11472–11481 (2018).
8. M. Garcia and V. Gruev, "Optical characterization of rigid endoscopes and polarization calibration methods," Opt. Express **25**, 15713–15728 (2017).
9. J. S. Tyo, D. L. Goldstein, D. B. Chenault, and J. A. Shaw, "Review of passive imaging polarimetry for remote sensing applications," Appl. Opt. **45**, 5453–5469 (2006).
10. M. Bass and V. N. Mahajan, *Handbook of Optics, Volume I: Geometrical and Physical Optics, Polarized Light, Components and Instruments* (McGraw-Hill, 2010).
11. J. Morrill, C. Korendyke, G. Brueckner, F. Giovane, R. Howard, M. Koomen, D. Moses, S. Plunkett, A. Vourlidas, and E. J. S. P. Esfandiari, "Calibration of the SOHO/LASCO C3 white light coronagraph," Solar Phys. **233**, 331–372 (2006).
12. T. Mu, D. Bao, C. Zhang, Z. Chen, and J. Song, "Optimal reference polarization states for the calibration of general Stokes polarimeters in the presence of noise," Opt. Commun. **418**, 120–128 (2018).
13. K. Twietmeyer and R. A. Chipman, "Optimization of Mueller matrix polarimeters in the presence of error sources," Opt. Express **16**, 11589–11603 (2008).
14. R. Azzam, I. Elminyawi, and A. El-Saba, "General analysis and optimization of the four-detector photopolarimeter," J. Opt. Soc. Am. A **5**, 681–689 (1988).
15. J. Zallat, S. Aïnouz, and M. P. Stoll, "Optimal configurations for imaging polarimeters: impact of image noise and systematic errors," J. Opt. A **8**, 807–814 (2006).
16. M. H. Smith, "Optimization of a dual-rotating-retarder Mueller matrix polarimeter," Appl. Opt. **41**, 2488–2493 (2002).
17. A. De Martino, Y.-K. Kim, E. Garcia-Caurel, B. Laude, and B. Drévillon, "Optimized Mueller polarimeter with liquid crystals," Opt. Lett. **28**, 616–618 (2003).
18. M. R. Foreman, A. Favaro, and A. Aiello, "Optimal frames for polarization state reconstruction," Phys. Rev. Lett. **115**, 263901 (2015).
19. G. Anna and F. Goudail, "Optimal Mueller matrix estimation in the presence of Poisson shot noise," Opt. Express **20**, 21331 (2012).
20. F. Goudail, "Optimal Mueller matrix estimation in the presence of additive and Poisson noise for any number of illumination and analysis states," Opt. Lett. **42**, 2153–2156 (2017).
21. F. Goudail, "Noise minimization and equalization for Stokes polarimeters in the presence of signal-dependent Poisson shot noise," Opt. Lett. **34**, 647–649 (2009).
22. J. S. Tyo, "Design of optimal polarimeters: maximization of signal-to-noise ratio and minimization of systematic error," Appl. Opt. **41**, 619–630 (2002).
23. A. N. Langville and W. J. Stewart, "The Kronecker product and stochastic automata networks," J. Comput. Appl. Math. **167**, 429–447 (2004).
24. J. S. Tyo and H. Wei, "Optimizing imaging polarimeters constructed with imperfect optics," Appl. Opt. **45**, 5497–5503 (2006).
25. F. Goudail and A. Bénière, "Estimation precision of the degree of linear polarization and of the angle of polarization in the presence of different sources of noise," Appl. Opt. **49**, 683–693 (2010).
26. J. Hough, "Polarimetry: a powerful diagnostic tool in astronomy," Astron. Geophys. **47**, 3.31–33.35 (2006).